SAIC-00/8006:APPAT-240
March 22, 2000

THE STRUCTURE AND DYNAMICS OF THE SOLAR CORONA AND INNER HELIOSPHERE

NASA SPACE PHYSICS THEORY CONTRACT NAS5-99018

FIRST QUARTER FIRST YEAR PROGRESS REPORT

Covering the period August 16, 1999 to November 15, 1999

Science Applications International Corporation

An Employee-Owned Company

Submitted by:

ZORAN MIKIC

PRINCIPAL INVESTIGATOR:

SCIENCE APPLICATIONS INTERNATIONAL CORPORATION

10260 CAMPUS POINT DRIVE

SAN DIEGO, CA 92121-1578

MARCH 22, 2000

FIRST QUARTER FIRST YEAR PROGRESS REPORT

This report covers technical progress during the first quarter of the first year of NASA Sun-Earth Connections Theory Program (SECTP) contract "The Structure and Dynamics of the Solar Corona and Inner Heliosphere," NAS5-99188, between NASA and Science Applications International Corporation, and covers the period August 16, 1999 to November 15, 1999. Under this contract SAIC and the University of California, Irvine (UCI) have conducted research into theoretical modeling of active regions, the solar corona, and the inner heliosphere, using the MHD model.

In the following sections we summarize our progress during this reporting period. Full descriptions of our work can be found in the cited publications, a few of which are attached to this report.

Publication on the August 11, 1999 Eclipse Prediction

Our publication for the proceedings of the conference "The Last Total Solar Eclipse of the Millennium," which was held in Istanbul, Turkey, August 13–15, 1999, has been completed (Mikić *et al.* 1999), and is included in the Appendix of this report. It discusses our 3D MHD modeling of the total solar eclipse that occurred on August 11, 1999, and a comparison between our model and observations.

Publication on the Modeling of the Solar Wind and Transition Region

Roberto Lionello presented a paper on "Magnetohydrodynamics of the Solar Corona and the Transition Region," at the *Meeting on Magnetic Fields and Solar Processes,* which was held in Florence, Italy, from September 12–18, 1999. The paper has appeared in the proceedings of this conference (Lionello, Linker, & Mikić 1999), and is included in the Appendix. An extended paper on this work is in preparation (Lionello, Linker, & Mikić 2000).

A New 3D MHD Code on Unstructured Tetrahedral Grids

We have developed a new algorithm for the solution of the time-dependent, resistive MHD equations in three-dimensional spatial domains of arbitrary shape and connectivity. The algorithm uses a finite-volume approach based on a primary grid of tetrahedral cells, and a secondary dual median grid. The resulting discrete operators preserve the annihilation properties of the divergence and curl, and lead to a compact, self-adjoint formulation. The discrete operators also minimize the same functionals as the original differential operators. The semi-implicit method of time advancement is used. The capability of mesh refinement and coarsening has also been built (but has not yet been tested). The algorithm is being implemented in F90 and MPI, and can be used on either single processor or massively parallel computers.

For initial testing purposes, we have used MH4D to solve the magnetic resistive equation and the scalar and vector advection equations. The flexibility and parallelism of MH4D is illustrated in Figure 1. We consider three of the many possible domain configurations (a cube,

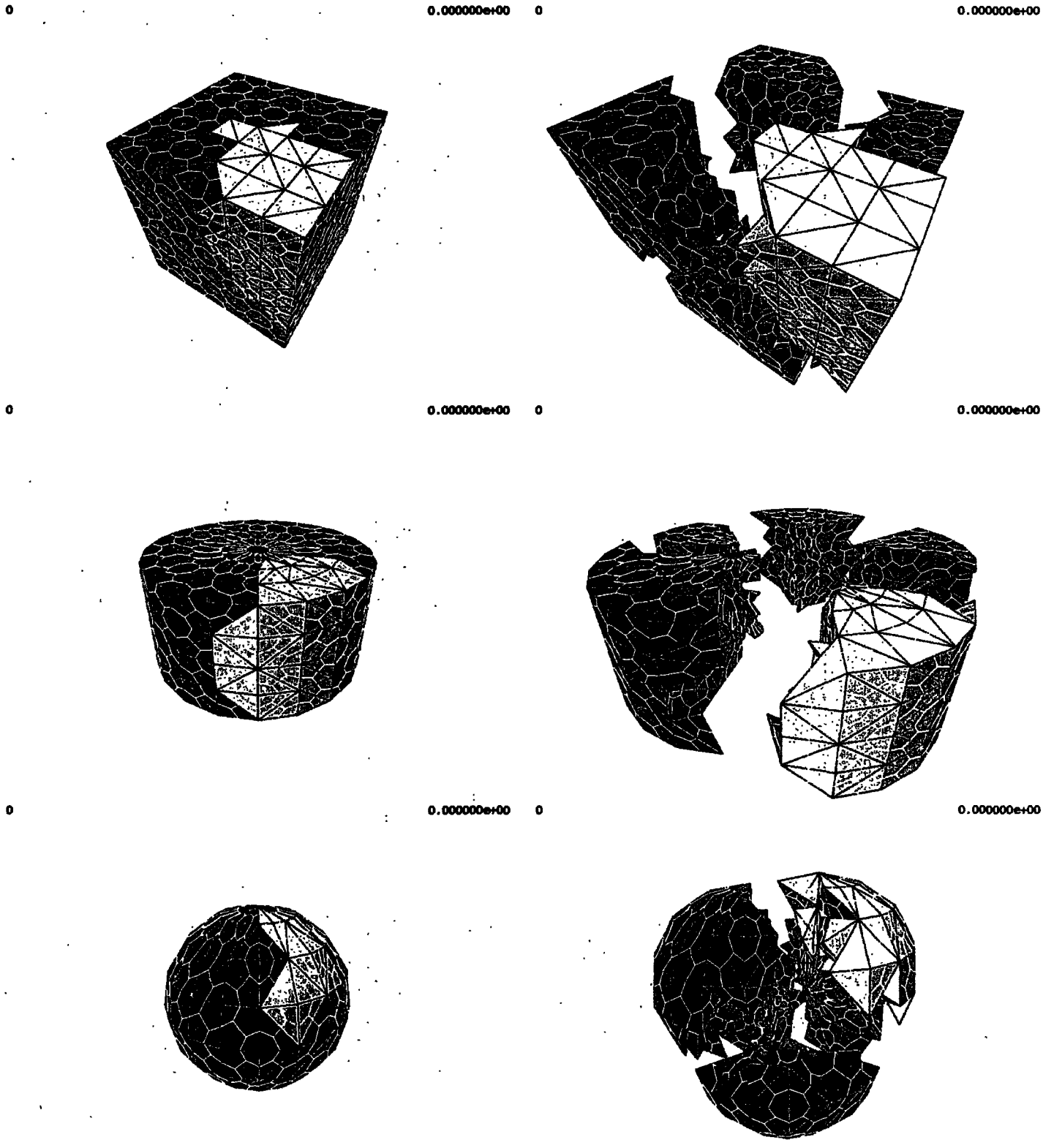

Figure 1. Decomposition of various spatial grids among 5 processors for the MH4D code. The code solves the MHD equations on an unstructured tetrahedral grid of arbitrary shape and connectivity. We show how the mesh is split between 5 processors for three illustrative domain configurations (a cube, a cylinder, and a sphere).

a cylinder, and a sphere), showing how the tetrahedral mesh is split between 5 processors. This code is presently being extended to solve the full MHD equations, and will be used in the future on a variety of solar and other MHD problems. The presentation "MH4D: A New Algorithm for Three-Dimensional MHD on an Unstructured Tetrahedral Grid," by R. Lionello and D. D. Schnack, was presented at the American Physical Society/Division of Plasma Physics Meeting, held in Seattle, WA, Nov. 15-19, 1999.

Comparing MHD Simulations of the Inner Heliosphere with Spacecraft Magnetic Field Measurements

Using the observed line-of-sight component of the photospheric magnetic field as input to a 3-dimensional MHD model, we have simulated the corona and heliosphere (out to 5 AU) for the time period known as "Whole Sun Month," August–September, 1996, which occurred shortly after the minimum of solar cycle 22. By flying simulated trajectories through the model, we can compare directly these results with interplanetary spacecraft observations. In Figure 2 we make such a comparison, using observations taken by the WIND and Ulysses spacecraft, which were widely separated in heliocentric distance, latitude, and longitude. Prior to this time, Ulysses was descending from higher to lower latitudes, and this rotation was the first time that Ulysses encountered significantly variable wind. Ulysses was located on the opposite side of the Sun from Earth, at a heliocentric distance of 4.25 AU and heliographic latitude of ~ N 28 degrees. In contrast, WIND was located in the ecliptic plane at 1 AU. The left column compares speed, scaled number density, and temperature at Ulysses, while the right column make the same comparison at WIND. In each panel, observations are colored blue and simulation results are red. At Ulysses, where the underlying profile consisted of a simple, single-stream pattern, the model appears to reproduce the essential features of the large-scale variations, i.e., the interaction region and the expansion wave. However, the interaction region is not as steep as the observations indicate, and the model does not mimic fluctuations on scales less than a few days. Nevertheless, when we consider that the measurements of the line-of-sight photospheric magnetic field used to drive the solution were always separated by ~ 180 degrees from the actual solar wind that Ulysses observed, the close agreement suggests that relatively little evolution of the corona took place, at least at latitudes of ~ 30 degrees. At WIND, there is a more complex pattern of variations that are only partially modeled by the MHD solution. The model predicts two fast (> 500 km/s) streams. Of these, one is found in the observations (at day 255), and the other (at day 240) might be related to the fast stream observed on day 243, although it is considerably broader. There are other minor perturbations in the model; however, none of them can be reliably matched with WIND observations. Overall, however, this comparison indicates that the model has reproduced the essential large-scale features of the heliosphere during this time period.

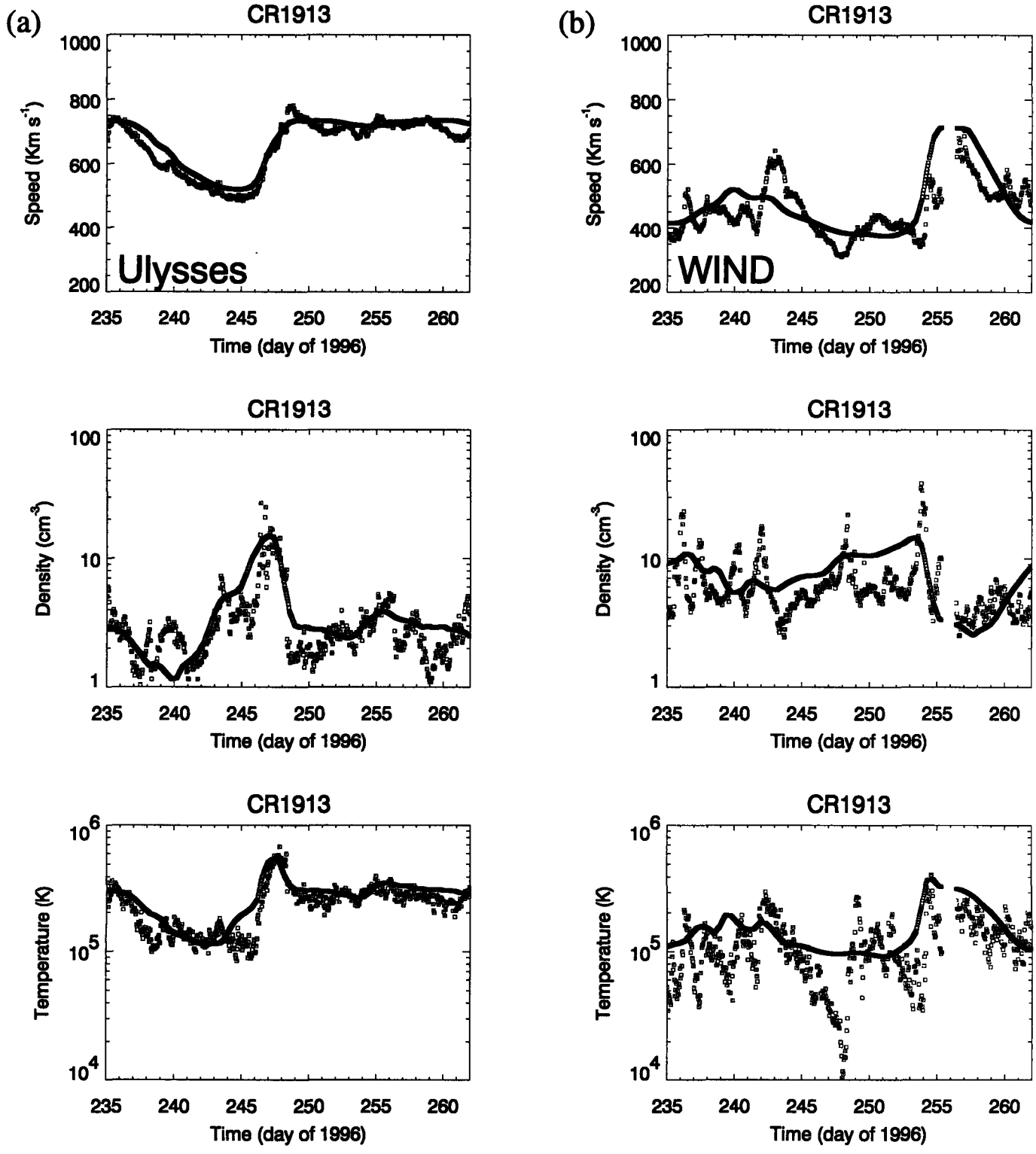

Figure 2. Comparison of Ulysses and WIND spacecraft measurements (blue) with 3D MHD simulations (red) during the Whole Sun Month time interval (August–September 1996). The Ulysses comparison is shown in the left panels; the WIND comparison is shown in the right panels.

Progress in Parallelizing the MAS Code

Optimization of Inter-Process Communication

The entire code has been carefully tested in order to avoid superfluous MPI communication calls. The size of the data sets to be sent/received in each communication call has been kept as large as possible by lumping together different arrays to maximize the communication efficiency.

In order to improve further the communication efficiency, different MPI communication protocols (that can be selected at run time via an input switch) have been introduced. In particular, the code can use "persistent communication routines" to reduce the overhead of repeated communication calls. Preliminary testing indicates a savings of up to 20% with respect the a more conventional coupled send/receive scheme. Since this performance-improvement can be problem dependent, further testing with different mesh sizes is required.

To better assess code performance, a measure of the latency time (time "wasted" while waiting for the processors to become synchronized) has been introduced. In the tests conducted so far, the latency time appears to be at least an order of magnitude smaller than the communication time.

Code Benchmarking

Careful benchmarking of the parallel version vs. the serial MAS code has been conducted for different test problems. The parallel version, when run on a single processor, produces restart files that agree perfectly (with no difference error) with the serial version. When run with more than one processor, the agreement with the serial version is maintained within machine roundoff accuracy. The origin of this difference has been tracked down to the non-associative nature of floating point additions.

Input-Controlled Problem Size

The scalar MAS code and the first parallel versions that have been derived from it do not allow the user to change the problem size (i.e., mesh dimensions) at run time. To change the problem size requires a re-compilation of the code. A new version has been developed that allows the choice of the grid size from the input file. As an important consequence, this upgrade removes the constraint that required the same number of mesh point on each processor. Full testing of this new feature will be performed after this version is integrated with new I/O scheme presently under development.

REFERENCES

Lionello, R., Linker, J. A., & Mikić, Z. 1999, in *Proc. of the 9th European Physical Society Meeting on Magnetic Fields and Solar Processes*, Florence, Italy (ESA SP-448), p. 1181.

Lionello, R., Linker, J. A., & Mikić, Z. 2000. "Magnetohydrodynamics of the Solar Corona and the Transition Region," in preparation.

Mikić, Z., Linker, J. A., Riley, P., & Lionello, R. 1999, "Predicting the Structure of the Solar Corona During the 11 August 1999 Total Solar Eclipse," in *The Last Total Solar Eclipse of the Millennium* (W. Livingston and A. Ö zgüç, eds.), Astronomical Society of the Pacific Conference Series, to appear.

APPENDIX

SELECTED REPRINTS

The Last Total Solar Eclipse of the Millennium
Proceedings of the Conference held in Istanbul, Turkey, 13-15 August 1999
W. Livingston and A. Özgüç, eds., ASP Conference Series, in press

Predicting the Structure of the Solar Corona During the 11 August 1999 Total Solar Eclipse

Zoran Mikić, Jon A. Linker, Pete Riley, and Roberto Lionello

Science Applications International Corporation, 10260 Campus Point Drive, San Diego, California 92121, U.S.A.

Abstract. We describe the application of a three-dimensional magnetohydrodynamic (MHD) model to the prediction of the structure of the corona during the total solar eclipse of 11 August 1999. The calculation uses the observed photospheric radial magnetic field as a boundary condition. This model makes it possible to determine the large-scale structure of the magnetic field in the corona, as well as the distribution of the solar wind velocity, plasma density, and temperature. The density was used to predict the plane-of-sky polarization brightness prior to the eclipse. The prediction is compared with an eclipse image taken in Turkey.

1. Introduction

Total solar eclipses offer an excellent opportunity to observe coronal streamers. During a total solar eclipse the moon blocks the bright light from the solar disk, so that the faint light scattered by the solar corona, which is more than a million times fainter than the photosphere, becomes visible. During totality the structures that characterize the white-light corona become visible, including prominences, helmet streamers, polar plumes, and coronal holes. Observers who witness a total solar eclipse invariably report that it is a beautiful sight to behold.

On 11 August 1999 a total solar eclipse occurred in Europe, the Middle East, and India. A partial eclipse was visible from the North-Eastern United States, and many parts of Europe, North Africa, and West Asia. (For an archive of past and future eclipse paths, see Fred Espenak's NASA eclipse home page.[1]) Fortunately, the viewing conditions were excellent in Harput, in Eastern Turkey, where one of us (ZM) successfully observed the eclipse.

In this paper we describe the a method of predicting the structure of the solar corona using a magnetohydrodynamic (MHD) model. By using this model it is possible to calculate the density in the corona, and thereby to deduce the brightness of coronal structures, given the observed magnetic field in the photosphere (a quantity that is measured routinely by several ground-based observatories). A description of the MHD model, as well as its application to the prediction of the structure of the corona during eclipses, is given by Mikić et al. (1999).

[1]See: `http://sunearth.gsfc.nasa.gov/eclipse/eclipse.html`

Previous comparisons of our results with coronal and interplanetary observations have shown that the large-scale structure of the solar corona is largely determined by the photospheric magnetic field distribution. It is remarkable that an MHD model, which incorporates the balance of magnetic, plasma, and gravity forces in equilibrium, can be used to estimate the large-scale distribution of plasma, magnetic field, and solar wind in the corona, using only the measured magnetic field in the photosphere.

This model can be used to make a prediction of the structure of the corona prior to eclipse day by using synoptic magnetic field measurements taken from the preceding solar rotation. After the calculation is performed, the white-light polarized brightness of the corona can be simulated from the MHD solution by integrating the electron density along the line of sight in the plane of the sky. This image can then be compared with coronal images taken during the eclipse. We published our prediction on the World Wide Web on 4 August 1999 (`http://haven.saic.com/corona/modeling.html`). Our prediction was updated and finalized on 6 August 1999, five days prior to the eclipse.

2. The MHD Model

Over the past decade we have developed a 3D MHD model of the corona and inner heliosphere. At present, we primarily use a polytropic MHD model for our large-scale calculations. This model, briefly described here, relies on a simple form of the energy equation (an adiabatic fluid with a reduced polytropic index). A more sophisticated model incorporating a more realistic description of the energy flow in the corona (including thermal conduction parallel to the magnetic field, radiation loss, coronal heating, and Alfvén wave acceleration) is under development (Mikić et al. 1999), and will be used in the future to improve our description of the corona and solar wind.

In the polytropic MHD model, the coronal plasma is described by the following equations:

$$\nabla \times \mathbf{B} = \frac{4\pi}{c}\mathbf{J}, \tag{1}$$

$$\nabla \times \mathbf{E} = -\frac{1}{c}\frac{\partial \mathbf{B}}{\partial t}, \tag{2}$$

$$\mathbf{E} + \frac{1}{c}\mathbf{v} \times \mathbf{B} = \eta \mathbf{J}, \tag{3}$$

$$\frac{\partial \rho}{\partial t} + \nabla \cdot (\rho \mathbf{v}) = 0, \tag{4}$$

$$\rho\left(\frac{\partial \mathbf{v}}{\partial t} + \mathbf{v} \cdot \nabla \mathbf{v}\right) = \frac{1}{c}\mathbf{J} \times \mathbf{B} - \nabla p + \rho \mathbf{g} + \nabla \cdot (\nu \rho \nabla \mathbf{v}), \tag{5}$$

$$\frac{\partial p}{\partial t} + \nabla \cdot (p\mathbf{v}) = -(\gamma - 1) p \nabla \cdot \mathbf{v}, \tag{6}$$

where $\mathbf{B}$ is the magnetic field, $\mathbf{J}$ is the electric current density, $\mathbf{E}$ is the electric field, ρ, $\mathbf{v}$, p, and T are the plasma mass density, velocity, pressure, and temperature, $\mathbf{g}$ is the gravitational acceleration, γ is the polytropic index, η is the

resistivity, and ν is the kinematic viscosity. The plasma pressure is $p = 2nkT$, where n is the electron and proton density, which are assumed to be equal. In the polytropic model, the complicated energy flow in the corona is modeled with a simple adiabatic energy equation with reduced γ (i.e., smaller than 5/3; see Parker 1963). The primary motivation for using a reduced γ is the fact that the temperature in the corona does not vary substantially (the limit $\gamma \to 1$ corresponds to an isothermal plasma). A typical choice, used here, is $\gamma = 1.05$.

We have developed a three-dimensional code to solve equations (1)–(6) in spherical coordinates (r, θ, ϕ) (Mikić & Linker 1994; Lionello, Mikić, & Schnack 1998). This code has been used extensively to model the 2D and 3D corona, including the structure of helmet streamers (Mikić & Linker 1996; Mikić, Linker & Schnack 1996; Linker et al. 1999), coronal mass ejections (Mikić & Linker 1994; Linker, Mikić, & Schnack 1994; Linker & Mikić 1995; Mikić & Linker 1997; Linker & Mikić 1997), and the long-term evolution of the solar corona and heliospheric current sheet (Mikić et al. 1999). Related techniques have been developed by Pneuman and Kopp (1971), Endler (1971), Steinolfson et al. (1982), Washimi, Yoshino, and Ogino (1987), Wang et al. (1993), Usmanov (1993, 1999), and Suess et al. (1999).

A boundary condition is imposed on the radial component of the magnetic field, B_r, at the lower corona ($r = R_s$). We use synoptic maps of the line-of-sight photospheric magnetic field measured at the National Solar Observatory at Kitt Peak (NSOKP) for this purpose. These photospheric magnetic field maps are built up from daily observations of the Sun during a solar rotation, and give a good approximation of the Sun's magnetic flux if the large-scale flux does not change considerably over a rotation. We also specify a uniform plasma density ($n_0 = 2 \times 10^8\,\mathrm{cm}^{-3}$) and temperature ($T_0 = 1.8 \times 10^6\,\mathrm{K}$) at $r = R_s$ in regions where the radial velocity is positive.

The application of the model is described by Mikić et al. (1999). Briefly, we start with a potential field in the corona (with $\nabla \times \mathbf{B} = 0$) that matches the measured field B_r at the base of the corona, and a transonic spherically symmetric solar wind solution (Parker 1963) to specify p, ρ, and $\mathbf{v}$. This initial nonequilibrium field is integrated in time until a steady state is reached. The final state has closed magnetic field regions (helmet streamers), where the solar wind plasma is trapped, surrounded by open fields (coronal holes), where the solar wind flows freely along magnetic field lines, accelerating to supersonic speeds.

3. The Prediction

Previous applications of our model to the prediction of the state of the solar corona were performed for eclipses that occurred close to solar minimum: the 3 November 1994 eclipse[2], which occurred during the declining phase of the last solar cycle; the 24 October 1995 and 9 March 1997 eclipses, which occurred at solar minimum, and the 26 February 1998 eclipse, which occurred during the

[2]We did not make a prediction for the 1994 eclipse. However, we compared eclipse images with a coronal model after the eclipse.

early rising phase of the new solar cycle. The 11 August 1999 eclipse presented a new challenge to our modeling efforts because it occurred during the late rising phase of the solar cycle on the approach to solar maximum. During this time, the solar magnetic field is significantly more complex than during solar minimum. The number of active regions is much larger, and the streamer structure in the corona is considerably more complex. A consequence for numerical modeling is the need for a significantly larger number of mesh points in the calculation to resolve coronal structures. Whereas our solar minimum calculations were performed on (r, θ, ϕ) grids with $81 \times 81 \times 64$ mesh points, in the present calculation we use $111 \times 141 \times 128$ mesh points. In addition, the large-scale magnetic field strength is larger, requiring smaller time steps. These calculations therefore took significantly longer to perform (90 CPU hours on a single processor of the T90 Cray supercomputer). We are presently developing a massively parallel version of our code which will enable us to perform these calculations in less time.

Using magnetic field measurements from a previous solar rotation for a prediction is expected to be a poorer approximation during this phase of the solar cycle than during solar minimum, when the large-scale structure of the Sun changes slowly between solar rotations. The photospheric magnetic field evolves more rapidly, making synoptic magnetic field measurements a less reliable approximation to the true state of the photospheric magnetic field. Figure 1 shows the evolution of the NSOKP photospheric magnetic field synoptic maps during the four solar rotations preceding the eclipse. Note that there is significant evolution of the magnetic field from rotation to rotation as active regions emerge and disperse. Figure 2 shows a comparison of a NSOKP synoptic map from June–July, 1999 with one near solar minimum (August–September, 1996), showing that the photospheric magnetic field is considerably more complex now. Consequently, the coronal magnetic field would be expected to be significantly more complex also. This expectation is confirmed by our results, described below.

The magnetic field is fitted at the solar poles using a smoothing procedure, since the line-of-sight component is not measured accurately there due to projection effects. Additionally, the data is smoothed everywhere, since the spatial resolution of the calculation is less than that of the measurements. The poor accuracy of the polar field (a limitation of the measurements) is expected to compromise our prediction more severely at this time of high solar activity, when active regions and coronal streamers are found at high latitudes, than at solar minimum.

On 28 July 1999 we started an MHD computation to predict the structure of the solar corona during the 11 August 1999 eclipse. We used NSOKP photospheric magnetic field measurements from Carrington rotation 1951 (corresponding to the dates 24 June–21 July, 1999). Figure 3 shows the raw NSOKP data and the smoothed data used in our calculation. It is apparent that the large-scale features in the magnetic field are reasonably well represented by the smoothed field.

Once the coronal solution reaches equilibrium, we use the density from the calculation to simulate the white-light polarized brightness of the corona on eclipse day. The polarized brightness is computed by integrating the electron

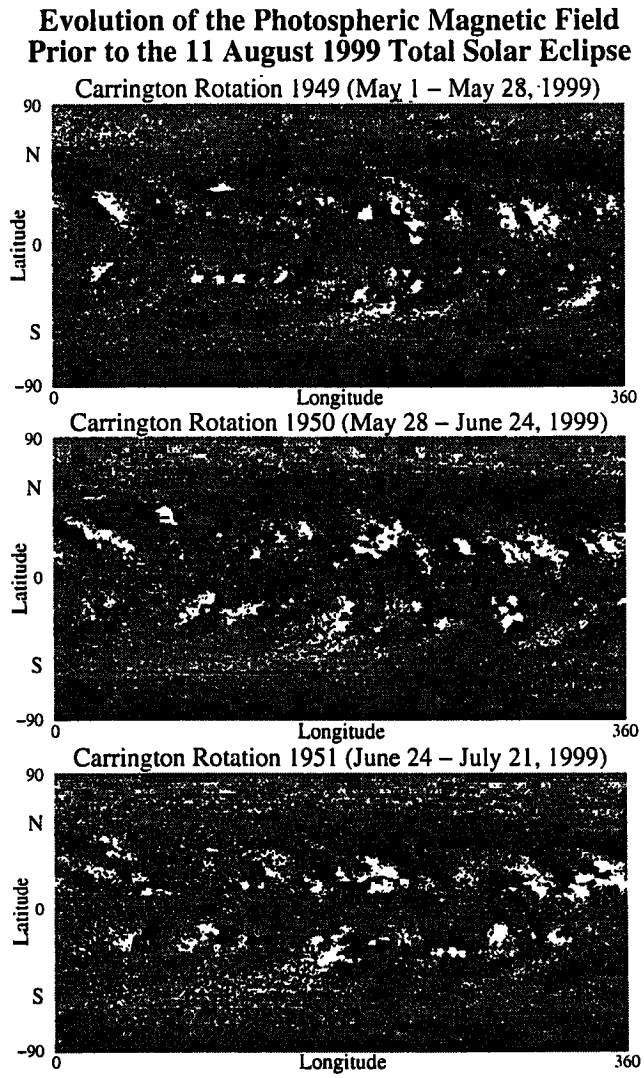

Figure 1. Synoptic maps of the radial component of the photospheric magnetic field for three solar rotations (Carrington rotations 1949–1951), as measured at the National Solar Observatory at Kitt Peak. Black shows fields directed into the Sun, whereas white shows fields directed out of the Sun. These maps show that the magnetic field is changing rapidly during the approach to the eclipse of 11 August 1999.

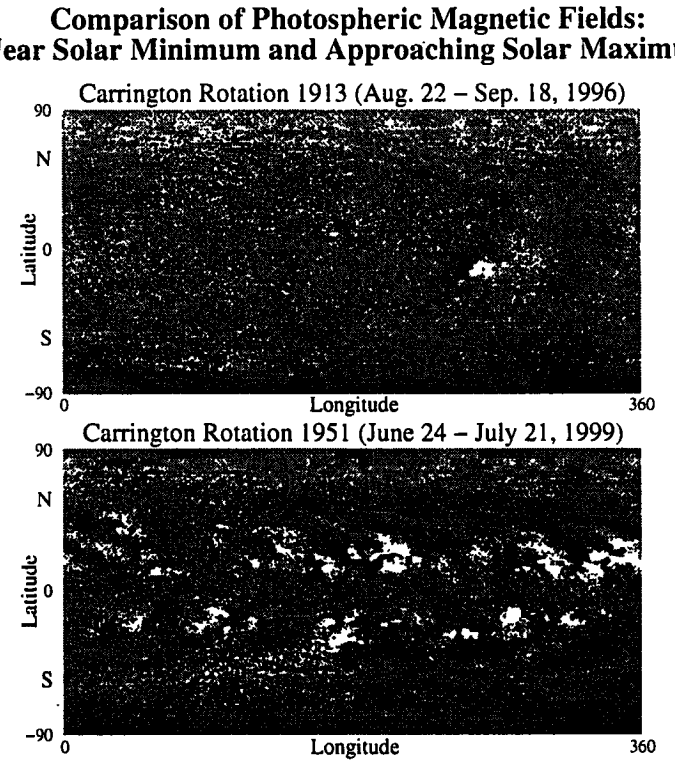

Figure 2. Synoptic maps of the radial component of the photospheric magnetic field near solar minimum (top) and approaching solar maximum (bottom).

density along the line of sight in the plane of the sky (convolved with a scattering function and filtered with a radial "vignetting function").

On 6 August 1999 we performed an updated calculation using the most recent magnetic field measurements available from NSOKP on that day, to incorporate the evolution of the magnetic field. The measurements used in the synoptic map were those from 13 July–5 August, 1999 (the synoptic map included Carrington longitudes 0°–107° from Carrington rotation 1951 and 107°–360° from rotation 1952). Due to time constraints, the updated calculation was performed on a coarser grid ($61 \times 71 \times 64$), and required 4 hours of CPU time. The results show that there are changes in the predicted coronal structure in the updated calculation. In particular, the position of some streamers changed perceptibly, and they had different tilts (especially near the west solar limb, where the magnetic field data was updated most significantly). However, the large-scale structure of the corona did not change dramatically. The updated calculation was not relaxed to steady state sufficiently, and the spatial resolution was inadequate, so that the results shown in this paper use the calculation with data for Carrington rotation 1951.

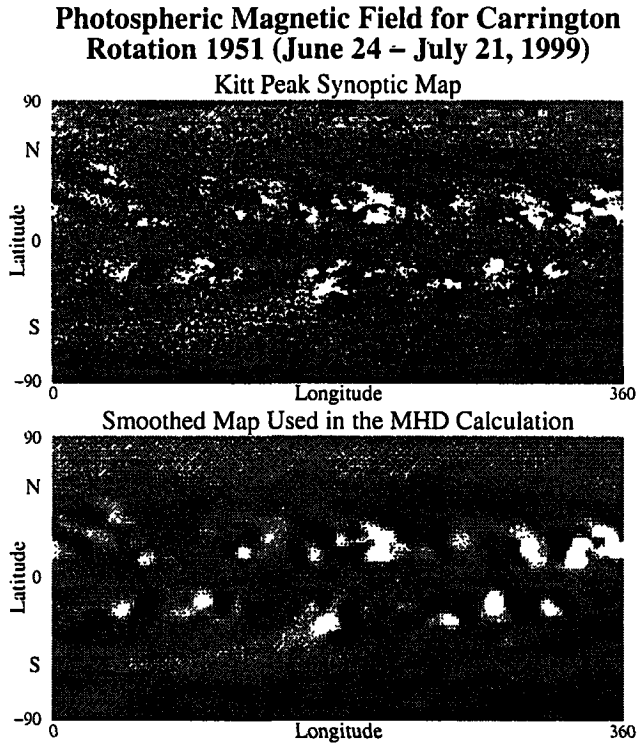

Figure 3. Synoptic map of the radial component of the photospheric magnetic field measured at the National Solar Observatory at Kitt Peak for Carrington rotation 1951 (top), and the smoothed version (bottom) that was used as a boundary condition for the MHD calculation for the eclipse prediction.

4. Comparison with an Eclipse Image

NASA astronomer Fred Espenak photographed the total solar eclipse on 11 August 1999 from Lake Hazar, Turkey. Twenty-two separate images with different exposures were combined digitally into a single composite image that more closely resembles the appearance of the solar corona as seen by the human eye (Espenak 1999). Additional photographs of the eclipse can be found on Fred Espenak's eclipse World Wide Web site.[3]

Figure 4 shows this eclipse image, as well as our predicted polarization brightness (pB) from the MHD model. The pB image was calculated from the simulated corona as it would appear in the plane of the sky on 11 August 1999, at 11:38 UT (corresponding to totality in Eastern Turkey), and has been radially detrended to account for the fall-off of coronal brightness with distance from the

[3]See: `http://www.mreclipse.com/TSE99reports/TSE99Espenak.html`

Comparison of a 3D MHD Coronal Prediction with an Image of the 11 August 1999 Total Solar Eclipse

Fred Espenak's Composite Image (Turkey)

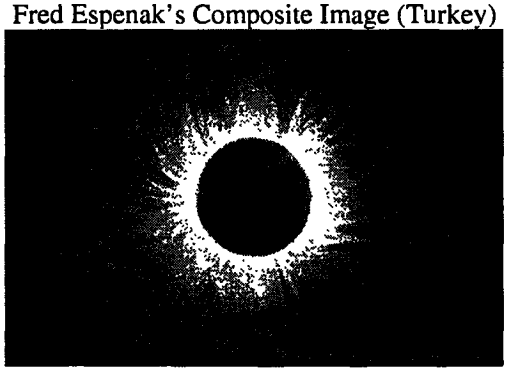

Predicted Polarization Brightness (MHD Model)

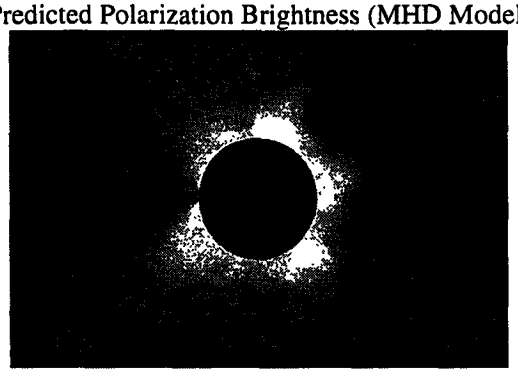

Predicted Magnetic Field Lines (MHD Model)

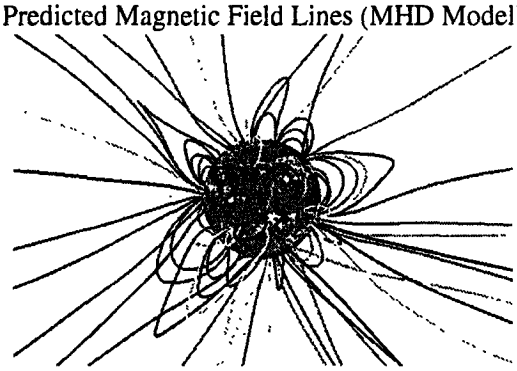

Figure 4. Comparison between a composite eclipse image created from photographs taken by Fred Espenak in Lake Hazar, Turkey (top) with the predicted polarization brightness of the simulated solar corona from our 3D MHD model (middle). The projected magnetic field lines from the model are also shown (bottom). Terrestrial (geocentric) north is vertically upward. (Solar north is 15° counterclockwise.) The eclipse image is copyrighted © 1999 by Fred Espenak.

Sun. This detrending is similar to the effect of combining various exposures in the composite eclipse image (although it is not an identical procedure), and is an attempt to reproduce the image seen by the human eye. Therefore, the agreement between the two images can only be expected to be qualitative at best; namely, the position and structure of streamers and coronal features ought to agree, but the brightness of individual features would not be expected to agree.

It is apparent that the eclipse image has considerably more fine structure than our prediction. This is primarily due to the limited spatial resolution of our calculation, but may also be due to the polytropic energy equation used in our model, and the fact that the fine-scale structure has been emphasized in the composite image (Espenak 1999). Note that the features that resemble "plumes," that are visible in the eclipse image at equatorial latitudes on the east solar limb, are not present in the model.

Previous comparisons of our simulations with Mauna Loa MK3 coronagraph observations on several days surrounding our solar minimum eclipse predictions have confirmed that the basic large-scale three-dimensional structure of the streamer belt is captured in our model (Linker et al. 1999). However, the agreement between our prediction and eclipse images as we approach solar maximum is not as good. The principal discrepancy seems to be in the tilt of the helmet streamers, and in the fact that we miss individual streamers, especially in the polar regions. Possible reasons for this discrepancy are discussed in the next section. Overall, however, the prediction gives a fair approximation to the state of the large-scale solar corona.

It is difficult to portray the complex three-dimensional structure of the solar corona for this simulation using still images. It is best seen in a movie of the polarization brightness during the whole solar rotation (Carrington rotation 1951), which can be found at our Web site.[4]

5. Discussion

During solar maximum the solar magnetic field is changing rapidly as new active regions emerge daily and disperse as they interact with existing active regions. The accuracy of an equilibrium model, which is based on synoptic magnetic field measurements, such as the one we describe, is therefore expected to be limited. Not surprisingly, the match between the prediction and actual observations is poorer during this time of high solar activity than it was during solar minimum. Furthermore, the failure to match the transverse component of the magnetic field (which is presently not measured), which specifies the "shear" in the field, and consequently the energization level of the coronal field (Mikić & Linker 1997), is expected to be most severe at solar maximum when the magnetic field is generally most active (and hence significantly "energized").

These two key approximations will be improved in future versions of our model. First, we now have the capability of running time-dependent simulations of the evolving solar corona as it responds to changes in the photospheric

[4]See: `http://haven.saic.com/corona/modeling.html`

magnetic field. In the future, we will be able to use daily magnetic field measurements to calculate the evolving solar corona. Second, current plans at Kitt Peak National Solar Observatory call for measurements of the vector magnetic field in the photosphere to be taken (the SOLIS project), which can be used in our model to match the transverse component of the magnetic field at the base of the corona (Mikić et al. 1999). A benefit of vector magnetic field measurements will be that polar fields will be more accurately determined (since the polar field, which is predominantly radial, will be measured as part of the transverse component). This can be expected to improve future predictions. Finally, our predictions will also be improved when our model with the more sophisticated energy equation becomes operational, and when we can perform higher-resolution calculations in less time with the massively parallel version of our code.

Acknowledgments. We wish to thank Dr. Jack Harvey at Kitt Peak National Solar Observatory for kindly providing us with up-to-date magnetic field data for our eclipse prediction. We thank Dr. Fred Espenak for use of his eclipse image. We thank Drs. Atila Özgüç and Tamer Atac for their hospitality and kindness during ZM's visit to Turkey. Kitt Peak synoptic magnetic data are courtesy of NSOKP, which is funded cooperatively by NSF/NOAO, NASA/GSFC, and NOAA/SEC. This research was supported by the NASA Space Physics Theory Program, the NASA Supporting Research and Technology Program, the NASA SOHO Guest Investigator Program, and NSF grant ATM-9613834. Computational facilities were provided by NSF at the San Diego Supercomputer Center.

References

Endler, F. 1971, Ph. D. Thesis, Gottingen University

Espenak, F. 1999, in this volume

Linker, J. A., & Mikić, Z. 1995, ApJ, 438, L45

Linker, J. A., & Mikić, Z. 1997, in Coronal Mass Ejections, Geophysical Monograph 99, ed. N. Crooker, J. Joselyn & J. Feynman (American Geophysical Union), 269

Linker, J. A., Mikić, Z., Biesecker, D. A., Forsyth, R. J., Gibson, S. E., Lazarus, A. J., Lecinski, A., Riley, P., Szabo, A., & Thompson, B. J. 1999, J. Geophys. Res., 104, 9809

Linker, J. A., Mikić, Z., & Schnack, D. D. 1994, in Proc. Third SOHO Workshop, SP-373, Solar Dynamic Phenomena and Solar Wind Consequences, Estes Park, Colorado, USA (European Space Agency), 249

Linker, J. A., Mikić, Z., & Schnack, D. D. 1996, in ASP Conf. Ser. Vol. 95, Solar Drivers of Interplanetary and Terrestrial Disturbances, ed. K. S. Balasubramaniam, S. L. Keil & R. N. Smartt (San Francisco: ASP), 208

Lionello, R., Mikić, Z., & Schnack, D. D. 1998, J. Comput. Phys., 140, 172

Mikić, Z., & Linker, J. A. 1994, ApJ, 430, 898

Mikić, Z., & Linker, J. A. 1996, in AIP Conf. Proc., 382, Solar Wind Eight: Proc. of the Eight Intl. Solar Wind Conf., ed. D. Winterhalter, J. T.

Gosling, S. R. Habbal, W. S. Kurth & M. Neugebauer (New York: AIP). 104

Mikić, Z., & Linker. J. A. 1997, in Coronal Mass Ejections. Geophysical Monograph 99, ed. N. Crooker, J. Joselyn & J. Feynman (American Geophysical Union), 57

Mikić, Z., Linker. J. A., Schnack. D. D., Lionello, R., & Tarditi, A. 1999, Phys. Plasmas. 6, 2217

Parker, E. N. 1963. Interplanetary Dynamical Processes (New York: Wiley-Interscience)

Pneuman, G. W., & Kopp, R. A. 1971, Sol. Phys., 18, 258

Steinolfson, R. S., Suess, S. T., & Wu, S. T. 1982. ApJ, 255, 730

Suess, S. T., Wang, A.-H., Wu, S. T., Poletto. G., & McComas, D. J. 1999, J. Geophys. Res.. 104, 4697

Usmanov, A. V. 1993, Sol. Phys., 146. 377

Usmanov, A. V. 1999, in AIP Conf. Proc., 471, Solar Wind Nine: Proc. of the Ninth Intl. Solar Wind Conf., ed. S. R. Habbal, R. Esser, J. V. Hollweg & P. A. Isenberg (New York: AIP), 397

Wang, A. H., Wu, S. T., Suess, S. T., & Poletto, G. 1993, Sol. Phys., 147, 55

Washimi, H., Yoshino, Y., & Ogino, T. 1987, Geophys. Res. Lett., 14, 487

MAGNETOHYDRODYNAMICS OF THE SOLAR CORONA AND THE TRANSITION REGION

Roberto Lionello, Jon A. Linker and Zoran Mikić
Science Applications International Corporation,
10260 Campus Point Dr.
San Diego, CA 92121-1578, USA
Ph: 1 (858) 826 6771
Fax: 1 (858) 826 6261
Email: lionel@iris023.saic.com

Abstract

The magnetic field dominates the structure of the solar corona. We have developed a magnetohydrodynamic model of the large scale structure and dynamics of the corona with a self-consistent treatment of the thermodynamics that includes radiation losses, thermal conduction along the magnetic field, and coronal heating. We specify a magnetic flux distribution on the solar surface and integrate the time dependent MHD equations to steady state. The model has been used to simulate the streamer/coronal hole configuration in two dimensions from the upper chromosphere and transition region to 30 $R_\odot$.

1 Introduction

The large scale structure and dynamics of the solar corona is dominated by the magnetic field. In the past the hydrodynamics and thermodynamics of the closed field regions (loops) of the corona has been studied with 1D models by many, amongst whom are [9], [5], [12], [10]. Other 1D models such as [14] and [3]. have been used to reproduce the solar wind in the open field regions. [8] successfully developed a 2D magnetohydrodynamic (MHD), isothermal model of the corona with a streamer and the open field regions. A 3D MHD, polytropic model could reproduce many features of the solar corona during Whole Sun Month [6]. However, since a simplified energy equation is used, it is not surprising that those models do not show the contrast in the plasma density and temperature between the open and closed field region and the contrast in speed between the fast and slow solar wind. [11] and [13] used a 2D MHD model of the corona and of the solar wind which includes heating and thermal conduction. In this paper we present a self-consistent study of the 2D large scale structure and dynamics of the solar corona and of the upper chromosphere. It has been obtained with an MHD numerical algorithm which treats the thermodynamics, including thermal conduction parallel to the magnetic field, radiation, and coronal heating. Thermal conduction is collisionally dominated in the inner corona, where it is calculated with Spitzer's formula, and smoothly becomes collisionless in the outer corona. The results show sharp gradients in the transition

Proc. 9th European Meeting on Solar Physics, 'Magnetic Fields and Solar Processes', Florence, Italy, 12-18 September 1999 (ESA SP-448, December 1999)

region, which appears structured according to the field topology. The temperature and density contrasts between the streamer and the poles are evident too. The aim of the present investigation has not been to reproduce the speed contrast between the fast and slow wind, which will be addressed with the same model at a later time.

2 The MHD and Thermodynamic Model

We have used our computational model to simulate the large scale structure of the 2D solar corona and the transition region in spherical coordinates (r, θ). Our model is capable to perform 3D simulations as well. It includes a self-consistent treatment of the magnetic, thermal and gravitational forces and of the energy transport. The physics is described in details in [7]. We solve the resistive and viscous MHD equations in spherical coordinates. The energy equation includes a radiation law function as in [1], thermal conduction along the magnetic field and coronal heating. Thermal conduction is collisional (Spitzer's law) for $R_\odot \leq r \lesssim 10\ R_\odot$ and smoothly becomes collisionless [4] for $r \gtrsim 10\ R_\odot$.

3 The Simulation

We have started our simulations by imposing an initial condition extracted from a 1D solution of a solar wind which includes the upper chromosphere and the transition region. A dipole field of 2.205 Gauss at the poles is prescribed as initial magnetic field. At the base of the domain, $r = 1\ R_\odot$, the magnetic flux corresponding to the aforementioned dipole is held fixed during the simulation. A fixed temperature of 2×10^4 K and a fixed density of 1.5×10^{10} cm^{-3} are also prescribed at the inner boundary. These values are compatible with those of the upper chromosphere. Characteristics equations are used to calculate the velocity along the magnetic field. These are also employed at the outer boundary (30 $R_\odot$), which is placed beyond the sonic and Alfvénic points. Because of the uncertainties surrounding coronal heating mechanisms, the heating in the energy equation is chosen to be a parameterized function

$$H_{\rm ch} = H_0 \exp[-(r - R_\odot)/\lambda]. \qquad (1)$$

In the present simulation heating has been specified uniform in θ and $\lambda = 0.7\ R_\odot$. H_0 is such that the heat flux at the base is 10^5 erg cm^{-2} s^{-1}. The Lundquist number we have used in the calculation is $S = 5 \times 10^4$, which is many order of magnitude smaller than the value in the corona. This is an inevitable drawback common to all numerical computations, which are limited by the grid resolution. The same argument applies in order to explain the choice of a finite viscosity ν, which corresponds to a viscous diffusion time $\tau_\nu = 3.33 \times 10^3\ \tau_A$, where $\tau_\nu = R_\odot^2/\nu$, $\tau_A = R_\odot/v_A$ is the Alfvén transit time, and v_A is the Alfvén speed. We have used a 201×301 nonuniform grid in (r, θ). Radial grid points are denser at the base of the domain, the ratio between mesh spacing at 30 $R_\odot$ and 1 $R_\odot$ being 2×10^4. The ratio between latitudinal mesh spacing at the pole and at the equator is 2. We have advanced the MHD equations and looked for a steady solution.

4 Results

During the simulation a considerable fraction of the closed magnetic lines of the initial dipole are progressively opened. The final configuration of the magnetic field features a helmet streamer with a cusp-like top surrounded by open field regions (see Fig. 1). A current sheet is formed on top of the streamer, as Fig. 2 shows.

Currents are present in the closed field region under the streamer as well. This is in

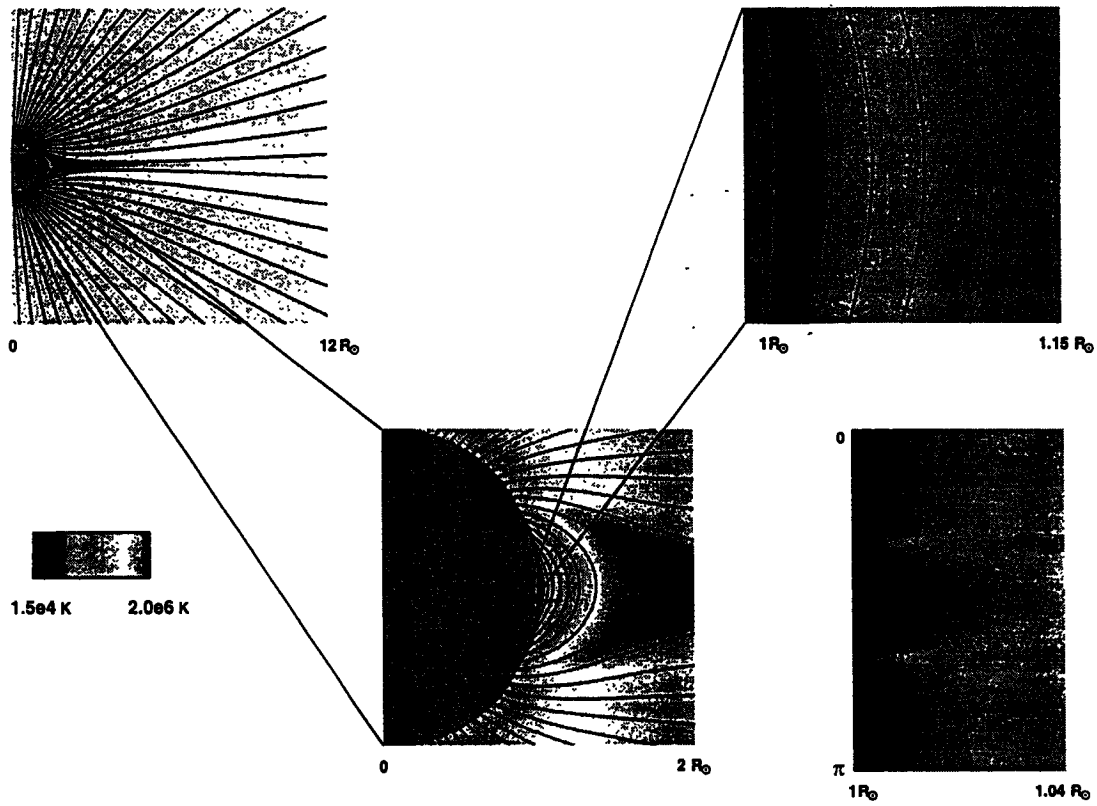

Figure 1: Plasma temperature at increasingly smaller scales with superimposed magnetic field lines. In the left corner, the temperature scale. In the right corner a Cartesian projection.

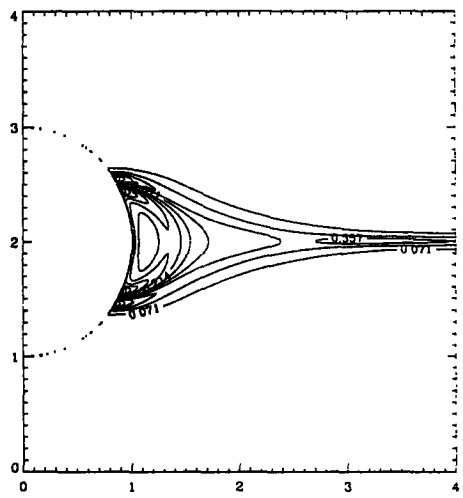

Figure 2: Current density contours at the end of the simulation. The helmet streamer and the heliospheric current sheet are visible.

contrast with the results obtained by [8], who found currents only at the boundary separating the streamer from the open field regions.

In Fig. 3a we plot the radial velocity as a function of the radius for the pole and the equator. The contrast between the two is indifferent. We have not included in this simulation a heating term dependent on the latitude and an additional source in the momentum equation, which are necessary to reproduce the fast and slow wind [13]. In fact the aim of this investigation is to study the 2D structure of the upper chromosphere, the transition region and the corona, and not to reproduce all the characteristics of the solar wind. Figures 3b and 3c show the particle number density and the temperature. A jump of several order of magnitudes is evident in the transition region in both cases. Notice that the equatorial region has higher temperature and density in the radial range corresponding to the streamer.

In Fig. 4a we plot three magnetic field lines representing a low lying loop. an intermediate

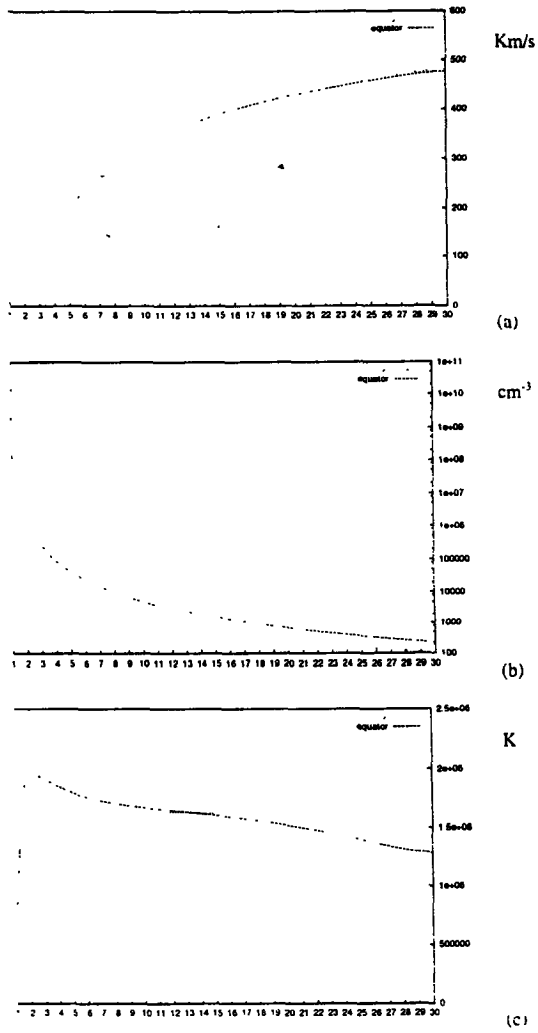

Figure 3: Radial velocity (a), particle number density (b), and temperature (c), as functions of the radial distance in solar radii for the equatorial and polar stream.

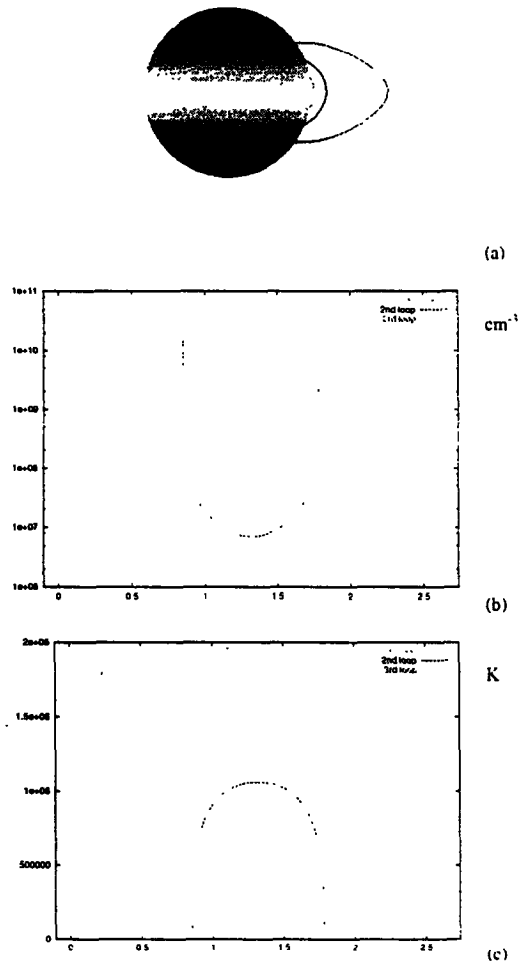

Figure 4: Three field lines (a) representing a low lying loop, an intermediate one, and the longest loop present in the simulation (on the solar surface the magnetic flux distribution is showed). Number densities (b) and temperature (c) as functions of the distance measured along the field lines.

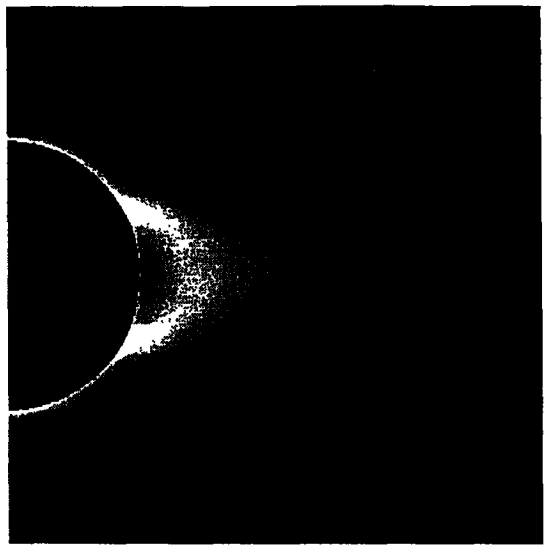

Figure 5: Polarized brightness image obtained from the data of the simulation.

loop, and a loop at the boundary between the open field region and the streamer. On the solar surface we show the magnetic flux distribution. Figure 4b has the densities for the three loops as function of the distance measured along the field lines. The temperature for the same loops is presented in Fig. 4c.

Figure 1 shows the temperature at increasingly smaller scales with superimposed magnetic field lines. The temperature maximum of about 2×10^6 K is in the closed field regions under the streamer, where hot plasma is trapped by the magnetic field. A projection in Cartesian coordinates shows that the height at which the transition region is found appears to be dependent on the latitude.

From our data we have produced a synthetic polarized brightness image (Fig. 5). The features can be compared with those present in real observations, taking into account that there is no occulting disk in our image.

5 Conclusion

We have been able to perform a two dimensional MHD simulation of the solar corona, the transition region and the upper chromosphere. This has been possible since our code includes a self consistent treatment of the thermodynamics with parallel thermal conduction, heating and radiation losses. It has been a very challenging computation, as the temperature, density and velocity span several orders of magnitude across very small scales ($\sim 10^{-3}$ $R_\odot$). The simulation has allowed us to investigate the large scale structure of the coronal magnetic field and underline the connections with the plasma properties. We have reproduced the helmet streamer surmounted by the heliospheric current sheet. The closed field regions below the helmet streamer appear to contrast in temperature and density with the open field regions, through which the solar wind flows. This seems to justify the presence of the currents in the closed field regions, where a Lorentz's force balancing the pressure gradients is needed. This is in contrast with [8], who however used the isothermal approximation in their model.

The transition region appears to be structured differently according to the magnetic field topology. In particular the height at which the temperature gradient rises is lower for the longest and hottest loops in the streamer than for the open field region and the shorter loops. This structure is also visible in a polarized light image, where the streamer gives the impression to possess two "legs".

With the present model we plan to study the 2D and 3D structure of the corona and of the solar wind. The latter can be modeled by prescribing a nonuniform heating functions and an additional momentum source in the calculation. Since our model includes the thermodynamics now, it may be possible to employ it to simulate prominence formation.

References

[1] Athay, R. G. 1986, Astrophys. J., 308, 975

[2] Bray, R. J. 1991, Plasma Loops in the Solar Corona, Cambridge; New York: Cambridge University Press

[3] Habbal, S. R., Esser, R., Guhathakurta, M., Fisher, R. 1995, Geophys. Res. Lett., 22, 1465

[4] Hollweg, J. V. 1978, Rev. Geophys. Space Phys., 16, 689

[5] Hood, A. W., and Priest, E. C., 1979, Astron. Astrophys., 77, 233

[6] Linker, J. A., Mikić, Z., Biesecker, D. A., Forsyth, R. J., Gibson, S. E., Lazarus, A. J., Riley, P., Szabo, A., Thompson, B. J. 1999, J. Geophys. Res., 104, 9809

[7] Mikić, Z., Linker, J. A., Schnack, D. D. , Lionello, R., and Tarditi, A. 1999, Phys. Plasmas, 6, 2217

[8] Pneuman, G. W., and Kopp R. A. 1971, Sol. Phys., 18, 258

[9] Rosner, R., Tucker, W. H., and Vaiana, G. S. 1978, Astrophys. J., 220, 643

[10] Serio, S., Peres, G., Vaiana, G. S., Golub, L., and Rosner, R., 1981, Astrophys. J., 243, 288

[11] Suess, S. T., Wang, A. H., Wu, S. T. 1996, J. Geophys. Res., 101, 19957

[12] Vesecky, J. F., Antiochos, S. K., and Underwood, J. H. 1979, Astrophys. J., 233, 987.

[13] Wang, A. H., Wu, S. T., Suess, S. T., and Poletto, G. 1998, J. Geophys. Res., 103, 1913

[14] Withbroe, G. L., 1988, Astrophys. J., 325, 442

REPORT DOCUMENTATION PAGE

Form Approved
OMB No. 0704-0188

Public reporting burden for this collection of information is estimated to average 1 hour per response, including the time for reviewing instructions, searching existing data sources, gathering and maintaining the data needed, and completing and reviewing the collection of information. Send comments regarding this burden estimate or any other aspect of this collection of information, including suggestions for reducing this burden, to Washington Headquarters Services, Directorate for Information Operations and Reports, 1215 Jefferson Davis Highway, Suite 1204, Arlington, VA 22202-4302, and to the Office of Management and Budget, Paperwork Reduction Project (0704-0188), Washington, DC 20506.

1. AGENCY USE ONLY (Leave Blank)	2. REPORT DATE	3. REPORT TYPE AND DATES COVERED
	March 22, 2000	1st Quarter 1st Year Progress Report (8/16/99 - 11/15/99)

4. TITLE AND SUBTITLE
"The Structure and Dynamics of the Solar Corona and Inner Heliosphere"
1st Quarter 1st Year Progress Report

5. FUNDING NUMBERS
NAS5-99188

6. AUTHORS
Zoran Mikic

7. PERFORMING ORGANIZATION NAME(S) AND ADDRESS(ES)
Science Applications International Corporation
10260 Campus Point Drive MSW2M
San Diego, CA 92121-1578

8. PERFORMAING ORGANIZATION REPORT NUMBER
SAIC-00/8006:APPAT-240

9. SPONSORING/MONITORING AGENCY NAME(S) AND ADDRESS(ES)
NASA Headquarters Operation Office
Goddard Space Flight Center
Greenbelt, MD 20771

10. SPONSORING/MONITORING AGENCY REPORT NUMBER

11. SUPPLEMENTARY NOTES

12a. DISTRIBUTION/AVAILABILITY STATEMENT

12b. DISTRIBUTION CODE

13. ABSTRACT *(Maximum 200 words)*
This report details progress during the first quarter of the first year of our Sun-Earth Connections Theory Program contract.

14. SUBJECT TERMS
Solar Corona, Coronal Magnetic Field, Heliosphere, Magnetohydrodynamics

15. NUMBER OF PAGES
25

16. PRICE CODE

17. SECURITY CLASSIFICATION OF REPORT	18. SECURITY CLASSIFICATION OF THIS PAGE	19. SECURITY CLASSIFICATION OF ABSTRACT	20. LIMITATION OF ABSTRACT
UNCLASSIFIED	UNCLASSIFIED	UNCLASSIFIED	UL

REPORT DOCUMENTATION PAGE

Form Approved
OMB No. 0704-0188

Public reporting burden for this collection of information is estimated to average 1 hour per response, including the time for reviewing instructions, searching existing data sources, gathering and maintaining the data needed, and completing and reviewing the collection of information. Send comments regarding this burden estimate or any other aspect of this collection of information, including suggestions for reducing this burden, to Washington Headquarters Services, Directorate for Information Operations and Reports, 1215 Jefferson Davis Highway, Suite 1204, Arlington, VA 22202-4302, and to the Office of Management and Budget, Paperwork Reduction Project (0704-0188), Washington, DC 20506

1. AGENCY USE ONLY (Leave Blank)	2. REPORT DATE	3. REPORT TYPE AND DATES COVERED
	March 22, 2000	1st Quarter 1st Year Progress Report (8/16/99 - 11/15/99)

4. TITLE AND SUBTITLE
"The Structure and Dynamics of the Solar Corona and Inner Heliosphere"
1st Quarter 1st Year Progress Report

5. FUNDING NUMBERS
NAS5-99188

6. AUTHORS
Zoran Mikic

7. PERFORMING ORGANIZATION NAME(S) AND ADDRESS(ES)

Science Applications International Corporation
10260 Campus Point Drive MSW2M
San Diego, CA 92121-1578

8. PERFORMAING ORGANIZATION REPORT NUMBER
SAIC-00/8006:APPAT-240

9. SPONSORING/MONITORING AGENCY NAME(S) AND ADDRESS(ES)

NASA Headquarters Operation Office
Goddard Space Flight Center
Greenbelt, MD 20771

10. SPONSORING/MONITORING AGENCY REPORT NUMBER

11. SUPPLEMENTARY NOTES

12a. DISTRIBUTION/AVAILABILITY STATEMENT

12b. DISTRIBUTION CODE

13. ABSTRACT *(Maximum 200 words)*

This report details progress during the first quarter of the first year of our Sun-Earth Connections Theory Program contract.

14. SUBJECT TERMS
Solar Corona, Coronal Magnetic Field, Heliosphere, Magnetohydrodynamics

15. NUMBER OF PAGES
25

16. PRICE CODE

17. SECURITY CLASSIFICATION OF REPORT	18. SECURITY CLASSIFICATION OF THIS PAGE	19. SECURITY CLASSIFICATION OF ABSTRACT	20. LIMITATION OF ABSTRACT
UNCLASSIFIED	UNCLASSIFIED	UNCLASSIFIED	UL